

# Symptomatic Carotid Plaques Demonstrate Less Leaky Plaque Microvasculature Compared With the Contralateral Side: A Dynamic Contrast-Enhanced Magnetic Resonance Imaging Study

Geneviève A. J. C. Crombag, MD; Raf H. M. van Hoof, PhD; Robert J. Holtackers, MSc; Floris H. B. M. Schreuder, MD; Martine T. B. Truijman, MD, PhD; Tobien A. H. C. M. L. Schreuder, MD; Narender P. van Orshoven, MD; Werner H. Mess, MD, PhD; Paul A. M. Hofman, MD, PhD; Robert J. van Oostenbrugge, MD, PhD; Joachim E. Wildberger, MD, PhD; M. Eline Kooi, PhD

**Background**—Rupture of a vulnerable carotid atherosclerotic plaque is an important underlying cause of ischemic stroke. Increased leaky plaque microvasculature may contribute to plaque vulnerability. These immature microvessels may facilitate entrance of inflammatory cells into the plaque. The objective of the present study is to investigate whether there is a difference in plaque microvasculature (the volume transfer coefficient  $K^{trans}$ ) between the ipsilateral symptomatic and contralateral asymptomatic carotid plaque using noninvasive dynamic contrast-enhanced magnetic resonance imaging.

**Methods and Results**—Eighty-eight patients with recent transient ischemic attack or ischemic stroke and ipsilateral >2 mm carotid plaque underwent 3 T magnetic resonance imaging to identify plaque components and to determine characteristics of plaque microvasculature. The volume transfer coefficient  $K^{trans}$ , indicative for microvascular density, flow, and permeability, was calculated for the ipsilateral and asymptomatic plaque, using a pharmacokinetic model (Patlak). Presence of a lipid-rich necrotic core, intraplaque hemorrhage, and a thin and/or ruptured fibrous cap was assessed on multisequence magnetic resonance imaging. We found significantly lower  $K^{trans}$  in the symptomatic carotid plaque compared with the asymptomatic side ( $0.057 \pm 0.002 \text{ min}^{-1}$  versus  $0.062 \pm 0.002 \text{ min}^{-1}$ ;  $P=0.033$ ). There was an increased number of slices with intraplaque hemorrhage ( $0.9 \pm 1.6$  versus  $0.3 \pm 0.8$ ,  $P=0.002$ ) and lipid-rich necrotic core ( $1.4 \pm 1.9$  versus  $0.8 \pm 1.4$ ,  $P=0.016$ ) and a higher prevalence of plaques with a thin and/or ruptured fibrous cap (32% versus 17%,  $P=0.023$ ) at the symptomatic side.

**Conclusions**— $K^{trans}$  was significantly lower in symptomatic carotid plaques, indicative for a decrease of plaque microvasculature in symptomatic plaques. This could be related to a larger amount of necrotic tissue in symptomatic plaques.

**Clinical Trial Registration**—URL: <http://www.clinicaltrials.gov.uk>. Unique identifier: NCT01208025. (*J Am Heart Assoc.* 2019;8:e011832. DOI: 10.1161/JAHA.118.011832.)

**Key Words:** angiogenesis • atherosclerosis • ischemic stroke • magnetic resonance imaging

Atherosclerosis of the carotid artery accounts for about one fifth of ischemic strokes.<sup>1</sup> Rupture of a vulnerable atherosclerotic plaque can lead to thromboemboli and, subsequently, to ischemic events.<sup>2–5</sup> During the past decade, it was demonstrated that patients with an increased stroke risk can be identified on the basis of plaque composition on

magnetic resonance imaging (MRI) rather than degree of stenosis.<sup>6,7</sup> These studies focused on the presence of intraplaque hemorrhage, a large lipid-rich necrotic core (LRNC), and thinning or rupture of the fibrous cap. In addition, angiogenesis is thought to play a key role in atherogenesis, but its exact role is still unclear. Plaque microvessels facilitate

From the Departments of Radiology and Nuclear Medicine (G.A.J.C.C., R.H.M.v.H., R.J.H., P.A.M.H., J.E.W., M.E.K.), Neurology (M.T.B.T., R.J.v.O.), and Clinical Neurophysiology (W.H.M.) and CARIM School for Cardiovascular Diseases (G.A.J.C.C., R.H.M.v.H., R.J.H., W.H.M., R.J.v.O., J.E.W., M.E.K.), Maastricht University Medical Centre, Maastricht, The Netherlands; Control Systems Technology, Department of Mechanical Engineering, Eindhoven University of Technology, Eindhoven, The Netherlands (R.H.M.v.H.); Department of Neurology, Donders Institute for Brain Cognition & Behaviour, Radboud University Medical Centre, Nijmegen, The Netherlands (F.H.B.M.S.); Department of Neurology, Zuyderland, Heerlen, The Netherlands (T.A.H.C.M.L.S.); Department of Neurology, Zuyderland, Sittard, The Netherlands (N.P.v.O.).

**Correspondence to:** M. Eline Kooi, PhD, Department of Radiology and Nuclear Medicine, Maastricht University Medical Centre, P.O. Box 5800, 6202 AZ Maastricht, The Netherlands. E-mail: [eline.kooi@mumc.nl](mailto:eline.kooi@mumc.nl)

Received January 16, 2019; accepted March 4, 2019.

© 2019 The Authors. Published on behalf of the American Heart Association, Inc., by Wiley. This is an open access article under the terms of the Creative Commons Attribution-NonCommercial-NoDerivs License, which permits use and distribution in any medium, provided the original work is properly cited, the use is non-commercial and no modifications or adaptations are made.

## Clinical Perspective

### What Is New?

- This study demonstrates, using dynamic contrast-enhanced magnetic resonance imaging, that there are fewer microvessels in the carotid symptomatic plaque compared with the contralateral asymptomatic plaque in symptomatic patients with carotid artery disease.

### What Are the Clinical Implications?

- Carotid plaque microvasculature is often considered as a vulnerable plaque characteristic; however, the present study demonstrates that the relation between plaque microvasculature and clinical symptom development is more complex.

leakage of red blood cells and inflammatory cells into the plaque tissue attributable to increased endothelial permeability and can thereby contribute to plaque destabilization.<sup>8–12</sup> Pharmacokinetic modeling of dynamic contrast-enhanced magnetic resonance imaging (DCE MRI) can be used to quantify plaque microvasculature noninvasively using pharmacokinetic modeling.<sup>13–18</sup> The pharmacokinetic parameter  $K^{trans}$  (volume transfer constant) is indicative for microvascular density, flow, and permeability.<sup>19,20</sup> A previous study showed a strong positive correlation between vessel wall  $K^{trans}$  with the microvessel endothelium density on histology ( $\rho=0.71$ ;  $P<0.001$ ) in 27 patients. We confirmed in 23 patients with recent ischemic stroke and  $>50\%$  carotid stenosis, scheduled for carotid surgery, that  $K^{trans}$  correlates well with histologic quantification of microvascular density ( $\rho$  between 0.59 and 0.65;  $P<0.003$ ).<sup>21,22</sup>

In vivo carotid plaque imaging gives the unique opportunity to study atherosclerotic plaques in patients noninvasively, which also enables one to study the plaque on the contralateral, asymptomatic side, which is usually not operated on and not often available for histologic studies.

Increased adventitial  $K^{trans}$  in carotid plaques is associated with cardiovascular ischemic events.<sup>23</sup> Although there was no difference between adventitial  $K^{trans}$  in symptomatic versus asymptomatic plaques in patients with cardiovascular events, the number of patients may have been too small to detect a significant difference, as only 7 contralateral, asymptomatic, carotid plaques were included in this analysis.<sup>23</sup>

The main objective of our study is to investigate whether there is a difference in microvasculature ( $K^{trans}$ ) between the ipsilateral symptomatic and contralateral asymptomatic carotid plaques in patients with a recent transient ischemic attack or ischemic stroke.

## Methods

For ethical reasons, the raw data that we collected cannot be made publicly available. The study was approved by the Medical Ethics Committee of the Maastricht University Medical Center, Maastricht, The Netherlands, under the condition that access to the data is granted only to (1) members of the research team, (2) the Medical Ethics Committee members who approved this study, and (3) authorized personnel of the Health Care Inspectorate. Hence, participants did not consent to publicly archiving their data. However, requests for anonymized data can be sent to Prof Dr Eline Kooi (eline.kooi@mumc.nl).

## Study Population

Patients with a recent ( $<3$  months) transient ischemic attack and/or ischemic stroke in the anterior circulation and an ipsilateral carotid artery plaque  $>2$  mm but  $<70\%$  stenosis were prospectively included.<sup>24</sup> Exclusion criteria were a probable cardiac source of the embolism, a clotting disorder, severe comorbidity, standard MRI contraindications, and a renal clearance  $<30$  mL/min. Institutional medical ethical committee approval was obtained, and all patients provided written informed consent. The degree of stenosis was determined with multidetector-row computed tomography based on the North American Symptomatic Carotid Endarterectomy Trial criteria.<sup>24</sup> Approval of the local Institutional Ethical Review Board was obtained, and written informed consent was obtained for all patients.

## Magnetic Resonance Imaging

Patients underwent an MRI examination on a 3 T system (Achieva; Philips Healthcare, Best, The Netherlands) using a dedicated 8-channel carotid radio frequency coil (Shanghai Chenguan Medical Technologies Co., Shanghai, China). A multisequence MRI protocol, as described previously,<sup>24</sup> was used and consisted of the following sequences: pre- and postcontrast T1 weighted (T1w) quadruple inversion recovery (QIR) turbo spin echo (TSE), 3-dimensional time of flight, T2 weighted (T2w) TSE, and 2-dimensional T1w inversion recovery turbo field echo.

In addition, for DCE MRI, an end-diastolic ECG-gated 3-dimensional T1 fast field echo MRI pulse sequence was acquired. The central slice was placed at the position with the highest plaque burden. The sequence consisted of the following parameters: repetition/echo time 11.6/5.7 ms, flip angle  $35^\circ$ , field of view  $130 \times 130$  mm, acquisition/reconstruction matrix  $208 \times 206/512 \times 512$ , 5 adjoining transversal slices, slice thickness 2 mm.<sup>20</sup> The temporal resolution was  $\approx 20$  seconds per time frame, depending on the heart rate. A

contrast medium, Gadobutrol (Gadovist, Bayer Healthcare, Berlin, Germany) using a dose of 0.1 mmol/kg body weight, was injected at the beginning of the third time frame. The contrast medium was injected with a power injector (Spectris Solaris, Medrad, Warrendale, PA) at a rate of 0.5 mL/s followed by a 20-mL saline bolus at that same rate. The DCE MRI acquisition was continued for 6 minutes after contrast injection.

## Magnetic Resonance Image Review

Magnetic resonance (MR) image review was performed by a trained observer with dedicated vessel wall analysis software (VesselMass, Leiden, The Netherlands)<sup>20</sup> blinded to clinical data and DCE MRI results. In case of doubt, a second highly experienced observer was consulted. The inner and outer vessel wall contours of the ipsilateral symptomatic carotid plaque and the contralateral plaque on all slice positions were delineated.

Per slice, luminal and outer vessel wall contours were drawn on the precontrast T1w QIR TSE, and in case of image artifacts on postcontrast T1w QIR TSE, or T2 weighted TSE MR images, in subsequent order. The DCE MR images were coregistered with the multisequence MR images. Image analysis was performed in the 5 slices that coregister with the 5 DCE MRI slices and also on all 15 multisequence MRI slices. The following aspects were assessed on the 5 MR slices that coregister to DCE MR images: presence of plaque (ie, maximum vessel wall thickness >1.5 mm), presence of a LRNC, intraplaque hemorrhage, and a thin and/or ruptured fibrous cap. The presence of a LRNC was defined as a region within the bulk of the plaque that did not show contrast enhancement on the postcontrast T1w QIR images. Presence of intraplaque hemorrhage was scored on T1w inversion recovery transient field echo images by the trained observer. Intraplaque hemorrhage was considered present in case of a hyperintense signal in the bulk of the plaque, compared with the sternocleidomastoid muscle and is considered as part of a LRNC. On the postcontrast T1w TSE image, the fibrous cap was defined as a high-signal area between the LRNC and the lumen of the carotid artery.<sup>25</sup> Fibrous cap status was dichotomized according to a previously published categorization.<sup>26</sup> When a continuous high-signal area between intraplaque hemorrhage and the lumen was identified, fibrous cap status was classified as being “intact and thick.” When no or an interrupted high-signal area was identified, fibrous cap status was classified as being “thin and/or ruptured.”

Luminal and outer vessel wall contours were transferred to the DCE MR images, and if necessary, contours were manually adjusted. The images acquired at each individual time frame were inspected, and these images were shifted to correct for small patient displacements during the dynamic acquisition, if necessary. To avoid partial volume effects, luminal contours

were corrected by keeping sufficient distance from the vessel lumen. When the adventitial vasa vasorum showed hyperenhancement after contrast material administration, outer plaque contours were corrected to include the adventitial vasa vasorum. The entire vessel wall region is defined as the region between the luminal and outer wall contours. The adventitial region of the vessel wall was defined according to previously described criteria,<sup>27</sup> that is, all pixels within 0.625 mm of the outer wall contour in a region of the vessel wall with plaque (ie, with a wall thickness >1.5 mm).

To evaluate potential differences in the positioning of the 5 DCE MRI slices with respect to the position with the largest plaque burden at the symptomatic and asymptomatic side, we identified the slice with the largest plaque burden at the symptomatic and asymptomatic side on the 15 adjoining 2-mm slices of the precontrast T1-weighted QIR TSE images. We compared this slice position to the position of the middle slice of the 5 DCE MRI slices.

## Pharmacokinetic Modeling

Pharmacokinetic parameters were estimated using the Patlak model<sup>28</sup> on a voxel-wise basis, as previously described,<sup>29</sup> with a phase-based population-averaged vascular input function determined in the carotid artery.<sup>20</sup> Shortly, contrast medium concentrations in the plaque were calculated from the signal intensity time course by using the Ernst equation on the basis of literature values for the longitudinal and transversal relaxation times of tissue<sup>30</sup> and the r1 and r2 relaxation rates of the contrast medium,<sup>31</sup> similar to previous studies.<sup>8,27,29,32</sup>

## Statistical Analysis

All calculations were made with SPSS version 23 (IBM Corporation, Armonk, NY). A  $P < 0.05$  was considered statistically significant. Data are presented as mean (plus or minus) standard deviation for normally distributed data or number (n) and percentage (%) for categorical data.

A paired-samples t test was used to investigate the differences in mean  $K^{\text{trans}}$  between the symptomatic and the contralateral asymptomatic plaque in each patient and to calculate differences in number of intraplaque hemorrhage and LRNC-positive slices as well as differences in distance between the slice with the largest plaque burden and the middle DCE MRI slice between the symptomatic and asymptomatic carotid artery. The difference in presence of intraplaque hemorrhage, LRNC, and fibrous cap status was investigated using a McNemar test. Mean vessel wall  $K^{\text{trans}}$  of plaques with and without an LRNC were compared using an independent-samples t test. Correlation between  $K^{\text{trans}}$  and time since last clinical event was evaluated using Spearman's correlation analysis for not normally distributed data.

## Results

We performed MRI in 112 patients. Fourteen patients were excluded because of low-quality ECG signal during scanning, 6 patients did not undergo an MRI examination (because of obesity [n=2] and claustrophobia [n=4]), and 4 patients were excluded because of insufficient DCE MR image quality. Eighty-eight patients,  $70.1 \pm 8.4$  years old and 63% males, were available for analysis. Baseline clinical characteristics are shown in Table 1.

Lower mean  $K^{\text{trans}}$  of the entire vessel wall was found for the ipsilateral symptomatic ( $0.057 \pm 0.0020 \text{ min}^{-1}$ ) versus the contralateral asymptomatic side ( $0.062 \pm 0.0017 \text{ min}^{-1}$ ) ( $P=0.033$ ). Mean  $K^{\text{trans}}$  of the adventitia did not differ between the 2 sides (symptomatic  $0.058 \pm 0.0020 \text{ min}^{-1}$  versus asymptomatic  $0.061 \pm 0.0028 \text{ min}^{-1}$ ;  $P=0.29$ ); see Figure and Table 2.

An overview of other plaque characteristics that are identified on multisequence MRI slices that coregister to the 5 DCE MRI slices is provided for the symptomatic and contralateral asymptomatic carotid artery in Table 2. The results show a significant difference in degree of stenosis ( $53.1 \pm 1.6$  versus  $42.5 \pm 1.6$ ;  $P < 0.001$ ) between the symptomatic and asymptomatic sides, as well as a significant higher prevalence of intraplaque hemorrhage (28% versus 14%;  $P=0.015$ ) and a thin and/or ruptured fibrous cap (32% versus 17%;  $P=0.023$ ) on the symptomatic side in at least 1 of the 5 multisequence MRI slices in the region covered by DCE MRI. An LRNC was present in this region on the symptomatic side in 41/88 (47%) patients and in 31/88 (35%) on the asymptomatic side ( $P=0.132$ ). Furthermore, there was a tendency for a lower  $K^{\text{trans}}$  of the entire vessel wall when a LRNC was present versus no LRNC ( $0.057 \pm 0.002 \text{ min}^{-1}$  versus  $0.061 \pm 0.003 \text{ min}^{-1}$ ,  $P=0.157$ ). The mean difference between the slice with the largest plaque burden and the

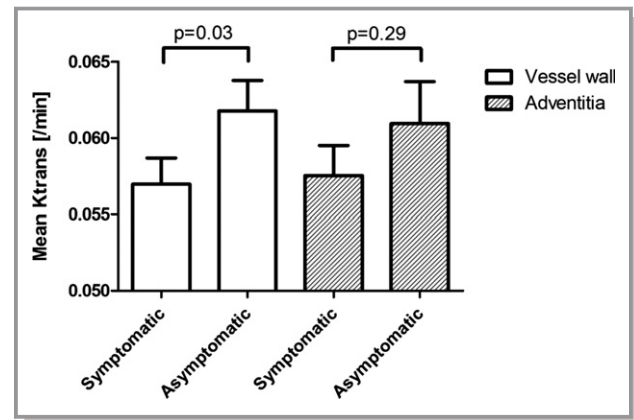


**Figure.** Boxplot showing the significant difference in vessel wall  $K^{\text{trans}}$  using a paired-samples t test between the symptomatic (mean  $\pm$  SEM;  $0.057 \pm 0.002 \text{ min}^{-1}$ ) and asymptomatic (mean  $\pm$  SEM;  $0.062 \pm 0.002 \text{ min}^{-1}$ ) side, with a  $P$  value of 0.03. There was no significant difference in adventitial  $K^{\text{trans}}$  between the symptomatic (mean  $\pm$  SEM;  $0.058 \pm 0.002 \text{ min}^{-1}$ ) and asymptomatic (mean  $\pm$  SEM;  $0.061 \pm 0.0017 \text{ min}^{-1}$ ) side, with a  $P$  value of 0.29.

middle slice of the DCE MRI coverage was not significantly different on the symptomatic and asymptomatic side ( $2.3 \pm 0.6$  versus  $3.1 \pm 0.7$  slices;  $P=0.472$ ).

On all 15 adjoining 2-mm multisequence MR images, there was a significantly higher prevalence of intraplaque hemorrhage (32% versus 15%;  $P=0.012$ ), and LRNC (55% versus 44%;  $P < 0.001$ ) on the symptomatic side; however, the prevalence of a thin or ruptured cap was not significantly different on the symptomatic versus asymptomatic side (39% versus 40%;  $P=1.0$ ).

The median time interval between carotid MRI and last clinical event was  $41 \pm 19$  days. There was no significant correlation between  $K^{\text{trans}}$  and the time since the last clinical event ( $\rho = -0.036$ ,  $P=0.739$ ).

**Table 1.** Patient Characteristics

Subjects, n (%)	88 (100)
Age, y	$70.1 \pm 8.4$
Male sex, n (%)	56 (63.6)
Body mass index, $\text{kg/m}^2$	$26.7 \pm 4.1$
Currently smoking, n (%)	16 (21.1)
Diabetes mellitus, n (%)	14 (18.2)
Hypertension, n (%)	50 (56.8)
Hypercholesterolemia, n (%)	38 (43.7)*
Statin use before most recent cerebrovascular event, n (%)	42 (47.7)*
Time between event and MRI, days	$41 \pm 19$

Data are presented as mean  $\pm$  SD or n (%). MRI indicates magnetic resonance imaging. \*One missing value.

## Discussion

This study shows a significantly lower  $K^{\text{trans}}$  of the entire plaque on the ipsilateral symptomatic side, compared with the contralateral asymptomatic side in 88 symptomatic patients with a recent transient ischemic stroke or ischemic stroke. There was no significant difference between symptomatic and asymptomatic plaques for adventitial  $K^{\text{trans}}$ . As expected, more slices with LRNC and intraplaque hemorrhage and a higher prevalence of a thin and/or ruptured fibrous cap were found in symptomatic plaques. Thus, the plaques at the symptomatic side were more complicated, and these plaques demonstrated fewer plaque microvessels.

Although our finding of less (leaky) plaque microvasculature in the entire vessel wall on the symptomatic side may



**Table 2.** Plaque Characteristics in the Symptomatic and Contralateral Asymptomatic Carotid Artery

n=88	Symptomatic Carotid Artery, n (%)	Asymptomatic Carotid Artery, n (%)	P Value
Degree of stenosis % ( $\pm$ SEM)	53.1 ( $\pm$ 1.6)*	42.5 ( $\pm$ 1.6)* <sup>†</sup>	<0.001*
Presence of lipid-rich necrotic core	41 (47)	31 (35)	0.175
Number of slices with lipid-rich necrotic core per patient	1.4 ( $\pm$ 1.9)	0.8 ( $\pm$ 1.4)	0.016*
Presence of intraplaque hemorrhage	25 (28)	12 (14)	0.015*
Number of slices with intraplaque hemorrhage per patient	0.9 ( $\pm$ 1.6)	0.3 ( $\pm$ 0.8)	0.002*
Thin and/or ruptured fibrous cap	25 (28)	12 (14)	0.023*
Plaque >1.5 mm on 5 of 5 slices	61 (69)	59 (67)	0.291
Plaque >1.5 mm on 4 of 5 slices	15 (17)	13 (15)	
Plaque >1.5 mm on 3 of 5 slices	7 (8)	5 (6)	
Plaque >1.5 mm on 2 of 5 slices	3 (3)	8 (9)	
Plaque >1.5 mm on 1 of 5 slice	1 (1)	3 (3)	
Plaque >1.5 mm on 0 of 5 slices	1 (1)	0 (0)	
Vessel wall $K^{\text{trans}}$ ( $\pm$ SEM)	0.057 ( $\pm$ 0.002)	0.062 ( $\pm$ 0.002)	0.033
Adventitial $K^{\text{trans}}$ ( $\pm$ SEM)	0.058 ( $\pm$ 0.002)	0.061 ( $\pm$ 0.003)	0.290

Assessed in the DCE MRI region (5 adjoining 2 mm slices).

\*Data missing for 7 patients.

<sup>†</sup>Statistically significant results.

seem contraindicated, as microvasculature is usually considered as a vulnerable plaque characteristic,<sup>33,34</sup> an earlier study also reported that  $K^{\text{trans}}$  in the entire vessel wall was not higher in symptomatic versus contralateral asymptomatic plaques.<sup>23</sup> In our study, the symptomatic plaques tended to have a higher prevalence of LRNC. In addition, we found a significant larger number of slices with LRNC on the symptomatic side. The LRNC consists of a large amount of necrotic tissue, which may explain fewer leaky microvessels in these plaques. The finding in the present study is also in line with a previous contrast-enhanced ultrasound study that detected plaque microvasculature in fibrous and fibro-fatty tissue, while plaque microvasculature was not observed in calcified, necrotic, and hemorrhagic tissue.<sup>35</sup> A large LRNC increases the risk for plaque rupture and subsequent clinical symptoms.<sup>36–39</sup>

In the adventitial region, no difference in  $K^{\text{trans}}$  between symptomatic and asymptomatic plaques was found, which is in concordance with a previous study that also reported no differences in adventitial  $K^{\text{trans}}$  between asymptomatic (n=7) and symptomatic carotid plaques (n=26) in patients with cerebrovascular events.<sup>23</sup> Previous studies have shown that the LRNC is mostly present in the intimal layer and hardly in the medial and adventitial layers, which may explain the lack of difference in microvasculature for the adventitial microvasculature.<sup>3,40</sup>

In the 2 previous studies by Wang et al, different parameters to study plaque microvasculature were used. Their first study used entire vessel wall  $K^{\text{trans}}$ ,<sup>41</sup> while the later study only reported adventitial  $K^{\text{trans}}$  values.<sup>23</sup> Therefore, we

reported both vessel wall  $K^{\text{trans}}$ , as well as adventitial  $K^{\text{trans}}$  values in the present study, similar to our previous studies<sup>22</sup> and in concordance with other DCE MRI studies.<sup>22,23,27,41</sup> Defining the adventitial region has been done using previously described criteria,<sup>22,27</sup> that is, all pixels within 0.625 mm of the outer wall contour in a region of the vessel wall with plaque (ie, with a wall thickness >1.5 mm). True differentiation between adventitia and media/intima remains challenging with MRI techniques.

Wang et al<sup>41</sup> demonstrated that  $K^{\text{trans}}$  in carotid plaques is associated with myocardial infarction and cerebrovascular events. Therefore, there may be a systemic increase in plaque microvasculature in patients with cardiovascular ischemic events.

We did find a significantly lower degree of stenosis, a lower prevalence of intraplaque hemorrhage, and a thin and/or ruptured fibrous cap on the contralateral carotid artery, which indicates less advanced atherosclerotic plaques on the asymptomatic side. Intuitively, one would expect a decrease in leaky plaque microvasculature and thus a lower vessel wall  $K^{\text{trans}}$  in less advanced lesions. However, our study demonstrated higher vessel wall  $K^{\text{trans}}$  on the asymptomatic compared with the symptomatic side. Therefore, it seems unlikely that the higher vessel wall  $K^{\text{trans}}$  is attributable to the lower degree of stenosis or the lower prevalence of intraplaque hemorrhage and a thin and/or ruptured fibrous cap on the asymptomatic side. This also indicates that the relation between  $K^{\text{trans}}$  and plaque vulnerability is complex, as symptomatic plaques are known to have a higher risk of future clinical events.

The rationale behind our study is to explore whether  $K^{trans}$  can contribute to a better risk stratification of patients with carotid atherosclerosis for surgical intervention. To be able to address the risk differences of plaques, plaque features (such as microvasculature) need to be reported on the whole plaque level and not on different regions of plaques. Therefore, we used the mean  $K^{trans}$  values, similar to previous studies.<sup>8,21–23,27,42</sup>

A strength of our study is the relatively large sample size compared with earlier DCE MRI studies of atherosclerotic plaques.<sup>23,27,41</sup> Our study has a number of limitations. First, because of the cross-sectional design of this study, no conclusion on causality can be drawn. Therefore, a possible causal relationship between plaque microvasculature and plaque symptomatology needs to be investigated in prospective studies. Second, the 2-dimensional DCE MRI sequence that was used in our study has a limited coverage in the longitudinal direction. During the MRI examination, the middle DCE MRI slice was positioned at the level with the largest plaque burden on the symptomatic side by visual inspection. We verified that there was no significant difference in distance between the slice with the largest plaque burden on the symptomatic and asymptomatic sides, respectively, and the middle DCE MRI slice. Third, we used fixed precontrast T1 and T2 relaxation times to convert vessel wall signal intensity into concentration. We chose this approach because a 3-dimensional sequence with high spatial resolution T1 mapping of the vessel wall was impractical in a clinical setting attributable to time, temporal resolution, and signal-to-noise constraints. A recent study described a multitasking approach for high-spatial-resolution, high-temporal-resolution DCE MRI including T1 mapping and large coverage of carotid arteries.

## Conclusion

The symptomatic carotid plaque shows a significantly lower  $K^{trans}$  for the entire vessel wall, indicative of a decrease of plaque microvasculature in symptomatic plaques. This may be related to a larger amount of necrotic tissue in symptomatic plaques. There was no significant difference in adventitial  $K^{trans}$  comparing the symptomatic with the asymptomatic side.

## Acknowledgments

The authors acknowledge the following participating centers: Laurentius Ziekenhuis, Roermond (AG Kortens); Viecuri Medisch Centrum, Venlo (BJ Meems); Zuyderland, Sittard/Heerlen (NP van Orshoven/AHCML Schreuder).

## Sources of Funding

This research was performed within the framework of CTMM, the Center for Translational Molecular Medicine ([www.ctmm.nl](http://www.ctmm.nl)), project PARISK (grant 01C-202), and supported by the Dutch Heart Foundation. This project received funding from the European Union (EU) Horizon 2020 Research and Innovation Programme under the Marie Skłodowska-Curie grant agreement No 722609. Wildberger and Kooi are supported by Stichting de Weijerhorst.

nl), project PARISK (grant 01C-202), and supported by the Dutch Heart Foundation. This project received funding from the European Union (EU) Horizon 2020 Research and Innovation Programme under the Marie Skłodowska-Curie grant agreement No 722609. Wildberger and Kooi are supported by Stichting de Weijerhorst.

## Disclosures

Wildberger receives institutional grants from AGFA, Bayer, GE, Philips, Siemens and is in the speaker's bureau for Bayer and Siemens (all outside the submitted work). The remaining authors have no disclosures to report.

## References

1. Chaturvedi S, Bruno A, Feasby T, Holloway R, Benavente O, Cohen SN, Cote R, Hess D, Saver J, Spence JD, Stern B, Wilterdink J; Therapeutics, Technology Assessment Subcommittee of the American Academy of Neurology. Carotid endarterectomy—an evidence-based review: report of the Therapeutics and Technology Assessment Subcommittee of the American Academy of Neurology. *Neurology*. 2005;65:794–801.
2. Gupta A, Baradaran H, Schweitzer AD, Kamel H, Pandya A, Delgado D, Dunning A, Mushlin AI, Sanelli PC. Carotid plaque MRI and stroke risk: a systematic review and meta-analysis. *Stroke*. 2013;44:3071–3077.
3. Virmani R, Burke AP, Farb A, Kolodgie FD. Pathology of the vulnerable plaque. *J Am Coll Cardiol*. 2006;47:C13–C18.
4. Yuan C, Zhang SX, Polissar NL, Echelard D, Ortiz G, Davis JW, Ellington E, Ferguson MS, Hatsukami TS. Identification of fibrous cap rupture with magnetic resonance imaging is highly associated with recent transient ischemic attack or stroke. *Circulation*. 2002;105:181–185.
5. Hosseini AA, Kandiyil N, Macsweeney ST, Altaf N, Auer DP. Carotid plaque hemorrhage on magnetic resonance imaging strongly predicts recurrent ischemia and stroke. *Ann Neurol*. 2013;73:774–784.
6. Saam T, Hetterich H, Hoffmann V, Yuan C, Dichgans M, Poppert H, Koeppel T, Hoffmann U, Reiser MF, Bamberg F. Meta-analysis and systematic review of the predictive value of carotid plaque hemorrhage on cerebrovascular events by magnetic resonance imaging. *J Am Coll Cardiol*. 2013;62:1081–1091.
7. Kwee RM, van Oostenbrugge RJ, Hofstra L, Teule GJ, van Engelshoven JM, Mess WH, Kooi ME. Identifying vulnerable carotid plaques by noninvasive imaging. *Neurology*. 2008;70:2401–2409.
8. Truijman MTB, Kwee RM, van Hoof RHM, Hermeling E, van Oostenbrugge RJ, Mess WH, Backes WH, Daemen MJ, Bucerius J, Wildberger JE, Kooi ME. Combined 18F-FDG PET-CT and DCE-MRI to assess inflammation and microvascularization in atherosclerotic plaques. *Stroke*. 2013;44:3568–3570.
9. McCarthy MJ, Loftus IM, Thompson MM, Jones L, London NJ, Bell PR, Naylor AR, Brindle NP. Angiogenesis and the atherosclerotic carotid plaque: an association between symptomatology and plaque morphology. *J Vasc Surg*. 1999;30:261–268.
10. Virmani R, Kolodgie FD, Burke AP, Finn AV, Gold HK, Tulenko TN, Wrenn SP, Narula J. Atherosclerotic plaque progression and vulnerability to rupture: angiogenesis as a source of intraplaque hemorrhage. *Arterioscler Thromb Vasc Biol*. 2005;25:2054–2061.
11. Sluimer JC, Daemen MJ. Novel concepts in atherogenesis: angiogenesis and hypoxia in atherosclerosis. *J Pathol*. 2009;218:7–29.
12. Sluimer JC, Gasc JM, van Wanroij JL, Kisters N, Groeneweg M, Sollewijn Gelpke MD, Cleutjens JP, van den Akker LH, Corvol P, Wouters BG, Daemen MJ, Bijlens AP. Hypoxia, hypoxia-inducible transcription factor, and macrophages in human atherosclerotic plaques are correlated with intraplaque angiogenesis. *J Am Coll Cardiol*. 2008;51:1258–1265.
13. Calcagno C, Mani V, Ramachandran S, Fayad ZA. Dynamic contrast enhanced (DCE) magnetic resonance imaging (MRI) of atherosclerotic plaque angiogenesis. *Angiogenesis*. 2010;13:87–99.
14. van Hoof RH, Heeneman S, Wildberger JE, Kooi ME. Dynamic contrast-enhanced MRI to study atherosclerotic plaque microvasculature. *Curr Atheroscler Rep*. 2016;18:33.

15. Kerwin W, Hooker A, Spilker M, Vicini P, Ferguson M, Hatsukami T, Yuan C. Quantitative magnetic resonance imaging analysis of neovasculature volume in carotid atherosclerotic plaque. *Circulation*. 2003;107:851–856.
16. Kerwin WS, Oikawa M, Yuan C, Jarvik GP, Hatsukami TS. MR imaging of adventitial vasa vasorum in carotid atherosclerosis. *Magn Reson Med*. 2008;59:507–514.
17. Lobbes MB, Heeneman S, Passos VL, Welten R, Kwee RM, van der Geest RJ, Wiethoff AJ, Caravan P, Misselwitz B, Daemen MJ, van Engelshoven JM, Leiner T, Kooi ME. Gadofosveset-enhanced magnetic resonance imaging of human carotid atherosclerotic plaques: a proof-of-concept study. *Invest Radiol*. 2010;45:275–281.
18. Chen H, Wu T, Kerwin WS, Yuan C. Atherosclerotic plaque inflammation quantification using dynamic contrast-enhanced (DCE) MRI. *Quant Imaging Med Surg*. 2013;3:298–301.
19. Calcagno C, Fayad ZA, Raggi P. Plaque microvascularization and permeability: key players in atherogenesis and plaque rupture. *Atherosclerosis*. 2017;263:320–321.
20. van Hoof RH, Hermeling E, Truijman MT, van Oostenbrugge RJ, Daemen JW, van der Geest RJ, van Orshoven NP, Schreuder AH, Backes WH, Daemen MJ, Wildberger JE, Kooi ME. Phase-based vascular input function: improved quantitative DCE-MRI of atherosclerotic plaques. *Med Phys*. 2015;42:4619–4628.
21. Kerwin WS, O'Brien KD, Ferguson MS, Polissar N, Hatsukami TS, Yuan C. Inflammation in carotid atherosclerotic plaque: a dynamic contrast-enhanced MR imaging study. *Radiology*. 2006;241:459–468.
22. van Hoof RHM, Voo SA, Sluimer JC, Wijnen NJA, Hermeling E, Schreuder F, Truijman MTB, Cleutjens JPM, Daemen M, Daemen JH, van Oostenbrugge RJ, Mess WH, Wildberger JE, Heeneman S, Kooi ME. Vessel wall and adventitial DCE-MRI parameters demonstrate similar correlations with carotid plaque microvasculature on histology. *J Magn Reson Imaging*. 2017;46:1053–1059.
23. Wang J, Chen H, Sun J, Hippe DS, Zhang H, Yu S, Cai J, Xie L, Cui B, Yuan C, Zhao X, Yuan W, Liu H. Dynamic contrast-enhanced MR imaging of carotid vasa vasorum in relation to coronary and cerebrovascular events. *Atherosclerosis*. 2017;263:420–426.
24. Truijman MTB, Kooi ME, van Dijk AC, de Rotte AAJ, van der Kolk AG, Liem MI, Schreuder FHBM, Boersma E, Mess WH, van Oostenbrugge RJ, Koudstaal PJ, Kappelle LJ, Nederkoorn PJ, Nederveen AJ, Hendrikse J, van der Steen AFW, Daemen MJAP, van der Lugt A. Plaque At RISK (PARISK): prospective multicenter study to improve diagnosis of high-risk carotid plaques. *Int J Stroke*. 2014;9:747–754.
25. Cai J, Hatsukami TS, Ferguson MS, Kerwin WS, Saam T, Chu B, Takaya N, Polissar NL, Yuan C. In vivo quantitative measurement of intact fibrous cap and lipid-rich necrotic core size in atherosclerotic carotid plaque: comparison of high-resolution, contrast-enhanced magnetic resonance imaging and histology. *Circulation*. 2005;112:3437–3444.
26. Takaya N, Yuan C, Chu B, Saam T, Underhill H, Cai J, Tran N, Polissar NL, Isaac C, Ferguson MS, Garden GA, Cramer SC, Maravilla KR, Hashimoto B, Hatsukami TS. Association between carotid plaque characteristics and subsequent ischemic cerebrovascular events: a prospective assessment with MRI—initial results. *Stroke*. 2006;37:818–823.
27. Sun J, Song Y, Chen H, Kerwin WS, Hippe DS, Dong L, Chen M, Zhou C, Hatsukami TS, Yuan C. Adventitial perfusion and intraplaque hemorrhage: a dynamic contrast-enhanced MRI study in the carotid artery. *Stroke*. 2013;44:1031–1036.
28. Patlak CS, Blasberg RG, Fenstermacher JD. Graphical evaluation of blood-to-brain transfer constants from multiple-time uptake data. *J Cereb Blood Flow Metab*. 1983;3:1–7.
29. Gaens ME, Backes WH, Rozel S, Lipperts M, Sanders SN, Jaspers K, Cleutjens JP, Sluimer JC, Heeneman S, Daemen MJ, Welten RJ, Daemen JW, Wildberger JE, Kwee RM, Kooi ME. Dynamic contrast-enhanced MR imaging of carotid atherosclerotic plaque: model selection, reproducibility, and validation. *Radiology*. 2013;266:271–279.
30. Stanisz GJ, Odorobina EE, Pun J, Escaravage M, Graham SJ, Bronskill MJ, Henkelman RM. T1, T2 relaxation and magnetization transfer in tissue at 3T. *Magn Reson Med*. 2005;54:507–512.
31. Pintaske J, Martirosian P, Graf H, Erb G, Lodemann KP, Claussen CD, Schick F. Relaxivity of gadopentetate dimeglumine (Magnevist), gadobutrol (Gadovist), and gadobenate dimeglumine (MultiHance) in human blood plasma at 0.2, 1.5, and 3 Tesla. *Invest Radiol*. 2006;41:213–221.
32. Kerwin WS, Liu F, Yarnykh V, Underhill H, Oikawa M, Yu W, Hatsukami TS, Yuan C. Signal features of the atherosclerotic plaque at 3.0 Tesla versus 1.5 Tesla: impact on automatic classification. *J Magn Reson Imaging*. 2008;28:987–995.
33. Moreno PR, Purushothaman KR, Fuster V, Echeverri D, Trusczyńska H, Sharma SK, Badimon JJ, O'Connor WN. Plaque neovascularization is increased in ruptured atherosclerotic lesions of human aorta: implications for plaque vulnerability. *Circulation*. 2004;110:2032–2038.
34. Dunmore BJ, McCarthy MJ, Naylor AR, Brindle NP. Carotid plaque instability and ischemic symptoms are linked to immaturity of microvessels within plaques. *J Vasc Surg*. 2007;45:155–159.
35. Vicenzini E, Giannoni MF, Puccinelli F, Ricciardi MC, Altieri M, Di Piero V, Gossetti B, Valentini FB, Lenzi GL. Detection of carotid adventitial vasa vasorum and plaque vascularization with ultrasound cadence contrast pulse sequencing technique and echo-contrast agent. *Stroke*. 2007;38:2841–2843.
36. Takaya N, Yuan C, Chu B, Saam T, Polissar NL, Jarvik GP, Isaac C, McDonough J, Natiello C, Small R, Ferguson MS, Hatsukami TS. Presence of intraplaque hemorrhage stimulates progression of carotid atherosclerotic plaques: a high-resolution magnetic resonance imaging study. *Circulation*. 2005;111:2768–2775.
37. Ota H, Yu W, Underhill HR, Oikawa M, Dong L, Zhao X, Polissar NL, Neradilek B, Gao T, Zhang Z, Yan Z, Guo M, Zhang Z, Hatsukami TS, Yuan C. Hemorrhage and large lipid-rich necrotic cores are independently associated with thin or ruptured fibrous caps: an in vivo 3T MRI study. *Arterioscler Thromb Vasc Biol*. 2009;29:1696–1701.
38. Cappendijk VC, Kessels AG, Heeneman S, Cleutjens KB, Schurink GW, Welten RJ, Mess WH, van Suylen RJ, Leiner T, Daemen MJ, van Engelshoven JM, Kooi ME. Comparison of lipid-rich necrotic core size in symptomatic and asymptomatic carotid atherosclerotic plaque: initial results. *J Magn Reson Imaging*. 2008;27:1356–1361.
39. Sun J, Underhill HR, Hippe DS, Xue Y, Yuan C, Hatsukami TS. Sustained acceleration in carotid atherosclerotic plaque progression with intraplaque hemorrhage: a long-term time course study. *JACC Cardiovasc Imaging*. 2012;5:798–804.
40. Nakashima Y, Fujii H, Sumiyoshi S, Wight TN, Sueishi K. Early human atherosclerosis: accumulation of lipid and proteoglycans in intimal thickenings followed by macrophage infiltration. *Arterioscler Thromb Vasc Biol*. 2007;27:1159–1165.
41. Wang J, Liu H, Sun J, Xue H, Xie L, Yu S, Liang C, Han X, Guan Z, Wei L, Yuan C, Zhao X, Chen H. Varying correlation between 18F-fluorodeoxyglucose positron emission tomography and dynamic contrast-enhanced MRI in carotid atherosclerosis: implications for plaque inflammation. *Stroke*. 2014;45:1842–1845.
42. Yuan J, Makris G, Patterson A, Usman A, Das T, Priest A, Teng Z, Hilborne S, Prudencio D, Gillard J, Graves M. Relationship between carotid plaque surface morphology and perfusion: a 3D DCE-MRI study. *MAGMA*. 2017;31:191–199.